NMR Studies of the Conformational Change in Human N-p21^{ras} Produced by Replacement of Bound GDP with the GTP Analog GTPγS†

Anne-Frances Miller,‡ Mary Z. Papastavros, and Alfred G. Redfield*

Department of Biochemistry, Brandeis University, Waltham, Massachusetts 02254

Received April 14, 1992; Revised Manuscript Received July 7, 1992

ABSTRACT: ^{1}H-Detected ^{15}N-edited NMR in solution was used to study the conformational differences between the GDP- and GTPγS-bound forms of human N-p21^{ras}. The amide protons of ^{15}N-labeled glycine and isoleucine were observed. Resonances were assigned to residues of particular interest, glycines-60 and -75 and isoleucines-21 and -36, by incorporating various ^{13}C-labeled amino acids in addition to [^{15}N]glycine and [^{15}N]iosleucine and by replacing Mg^{2+} by Co^{2+}. When GTPγS replaced GDP in the active site of p21^{ras}, only 5 of the 14 glycine amide resonances show major shifts, indicating that the conformational effects are fairly localized. Responsive glycines-10, -12, -13, and -15 are in the active site. Gly-75, located at the far end of a conformationally-active loop and helix, also responds to substitution of GTPγS for GDP, while Gly-77 does not, supporting a role for Gly-75 as a swivel point for the conformational change. The amide proton resonances of isoleucines-36 and -21 and a third unidentified isoleucine also undergo major shifts upon replacement of GDP by GTPγS. Thus, the effector-binding loop containing Ile-36 is confirmed to be involved in the conformational change, and the α-helix containing Ile-21 is also shown to be affected.

Human p21^{ras}'s are small guanine nucleotide-binding proteins (Bourne et al., 1991). p21^{ras}-related proteins function in cell signaling, proliferation, and differentiation (Barbacid, 1987; Bourne et al., 1990; Nishimura & Sekiya, 1987). In addition, p21^{ras} is a useful model for guanine nucleotide-binding proteins in general.

p21^{ras} cycles between its active guanosine 5′-triphosphate (GTP)[1] form and its inactive GDP form by hydrolysis of GTP, and by subsequent exchange of GDP for predominant GTP (Bourne et al., 1990; Field et al., 1987). GTPase activating protein (GAP) stimulates p21^{ras}'s GTP hydrolysis rate by 3 orders of magnitude (Trahey & McCormick, 1987), and exchange factor proteins interact with p21^{ras} to accelerate nucleotide exchange (West et al., 1990; Wolfman et al., 1990). Thus, various proteins normally regulate the balance between GDP- and GTP-bound p21^{ras} in cells. Because these proteins interact specifically with either the GTP- or the GDP-bound state of p21^{ras} (Field et al., 1987; Vogel et al., 1988), conformational differences between the two states are essential to the function of p21^{ras}.

Amino acids involved in the conformational switch of p21^{ras} have been identified. Residues 32–40 of the effector-binding loop are required for signal transduction from GTP-bound p21^{ras} (Willumsen et al., 1986; Sigal et al., 1986) and binding to GAP (Adari et al., 1988; Calés et al., 1988). The crystal structures of the GDP-bound and GTP analog-bound states of p21^{ras} differ significantly between residues 30–40 and 60–76 (Wittinghofer & Pai, 1991; Milburn et al., 1990), but apart from these changes and changes in hydrogen bonds directly involving the additional phosphate present in GTP analogs, the overall structures of GDP- and GMPPNP-bound p21^{ras} appear to be similar. NMR studies comparing p21^{ras} bound to GDP and to the GTP analog GTPγS have indicated that interactions between β-strands 2 and 3 evident in the GDP-bound state are altered in the GTPγS-bound state (Yamasaki et al., 1989).

NMR studies in this laboratory have identified the amide proton resonances of residues 10–16 in the phosphate-binding loop of N-p21^{ras} (Campbell-Burk et al., 1989; Redfield & Papastavros, 1990). The resonances of Gly-13 and Lys-16 occur at unusually low field due to the involvement of these protons in strong hydrogen bonds with the phosphate groups of GDP (Pai et al., 1989; Redfield & Papastavros, 1990). In this report, we have added to these assignments and extended them to residues more distant from the active site.

We have used isotope-editing NMR methods (Griffey & Redfield, 1987) in conjunction with ^{15}N-labeling of glycine and isoleucine to obtain highly simplified spectra containing only resonances from the amide protons of those amino acids. GTPγS was chosen for this work because of its high affinity for p21^{ras}, approaching those for GDP and GTP (Feuerstein et al., 1989), and because it is hydrolyzed by p21^{ras}, albeit at a reduced rate which is compatible with NMR experiments (Feuerstein et al., 1989). Thus, we expect that the p21^{ras}–GTPγS complex retains key characteristics of the p21^{ras}–GTP complex.

We have used ^{15}N-labeled glycine and isoleucine to report on conformational effects in the phosphate-binding loop and active site of p21^{ras}, and the effector-binding loop. Conserved glycines in the active site are essential to the function of p21^{ras} (Seeburg et al., 1984; Bos et al., 1985; Fasano et al., 1984). Ile-36 is central to the effector-binding loop and is conserved among p21^{ras}-related proteins (Bourne et al., 1991). According to the X-ray structures, the conformation of Ile-36 is coupled

† This work was supported in part by USPHS Grants CA51992 and GM20168. A.-F.M. is a Bristol-Myers Squibb Fellow of the Life Sciences Research Foundation and also gratefully acknowledges the Natural Sciences and Engineering Research Council of Canada for support during earlier stages of this research.

‡ Present address: Department of Chemistry, The Johns Hopkins University, Baltimore, MD 21218.

[1] Abbreviations: DTT, dithiothreitol; EDTA, ethylenediaminetetraacetic acid; GDP, guanosine 5′-diphosphate; GMPPCP, guanosine 5′-(β,γ-methylene)diphosphonate; GMPPNP, 5′-guanylyl imidodiphosphate; GTP, guanosine 5′-triphosphate; GTPγS, guanosine 5′-*O*-(3-thiotriphosphate); HEPES, 4-(2-hydroxyethyl)-1-piperazineethanesulfonic acid; HMQC, heteronuclear multiple quantum coherence; HSMQC, heteronuclear single and multiple quantum coherence; IPTG, isopropyl β-D-thiogalactopyranoside; OD, optical density at 660 nm, A_{660}; NMR, nuclear magnetic resonance; PAGE, polyacrylamide gel electrophoresis; PMSF, phenylmethanesulfonyl fluoride; SDS, sodium dodecyl sulfate; TLC, thin-layer chromatography; Tris, tris(hydroxymethyl)aminomethane.

0006-2960/92/0431-10208$03.00/0

to p21^{ras}'s ligation state (GDP vs GTP analogs) by Ile-36's direct linkage to Thr-35, which in turn hydrogen-bonds to the γ-phosphate of GTP (Pai et al., 1990; Milburn et al., 1990). Ile-55 serves as a probe of the β-pleated sheet of p21^{ras}, and isoleucines-21 and -24 report on effects on α-helix 1.

The Mg^{2+} ion of p21^{ras} could also mediate conformational effects, as some of the amino acids bound directly or indirectly to Mg^{2+} differ in the GDP and GTP forms of p21^{ras}. Our exploratory metal ion replacement experiments suggest that the protein conformation is sensitive to the identity of the metal ion.

MATERIALS AND METHODS

^{13}C- and ^{15}N-labeled amino acids were purchased from Cambridge Isotope Laboratories, except for [^{13}C]threonine. GTPγS (>80%) was obtained from Sigma on dry ice and used promptly. The colorimetric protein assay used was that of Bio-Rad. QA52 ion-exchange resin was from Whatman BioSystems Ltd., and Sephadex G-75 gel filtration resin was from Sigma Chemical Co. PD10 Sephadex G-25M columns were obtained from Pharmacia. Centricon-10 microconcentrators were from Amicon. The poly(ethyleneimine)–cellulose thin-layer chromatography plates used were Polygram 0.1-mm cel 300 PEI/UV_{254} from Sybron/Brinkman.

Threonine labeled in the carbonyl and C_α positions was synthesized according to Sato et al. (1957). The product was found to contain both threonine and allothreonine by thin-layer chromatography and NMR, in a ratio of 2.9 to 1 on the basis of ^1H and ^{13}C NMR. This synthesis also produced both the L and D isomers of both allothreonine and threonine. Therefore, L-threonine was estimated to comprise approximately three-eights of the product by weight, and 0.3 g of the product was used for 1 L of bacterial growth medium instead of the 0.12 g/L unlabeled threonine usually used in our growth media.

Plasmids. The gene for full-length human N-p21^{ras} was carried on pTrc99C (Amann et al., 1988) and expressed under control of the trc promoter (similar to the tac promoter; Amann et al., 1988). The gene for truncated N-p21^{ras}, coding for residues 1–166, was similarly expressed from the trc promotor in pTrc99C (this construction was made by J. A. Noble, Chiron Co.). The vector pTrc99C is a lac I^q and ampicillin resistance-bearing derivative of pKK233-2 (Amann & Brosius, 1985).

Escherichia coli Strains and Culture. When p21^{ras} was to be fully labeled with ^{15}N, DH5α was the host strain of *E. coli* used (Hanahan, 1983). Cells were grown to an OD of 1.6 in M9 medium, pelleted, and resuspended to an OD of 0.8 in fresh medium containing $^{15}NH_4Cl$ and 1 mM IPTG. The labeled culture was harvested after approximately 20 h at an OD of approximately 3.

When p21^{ras} was to be labeled with ^{15}N-labeled (and ^{13}C-labeled) amino acids, the polyauxotrophic strains of *E. coli* DL39 AvtA::Tn5 (avtA::Tn5 aspC ilvE tyrB; LeMaster & Richards, 1988; Muchmore et al., 1989) or DL39TG (aspC ilvE tyrB glyA::Tn5 Thr-34::Tn10; LeMaster & Richards, 1988) were used as previously described (Campbell-Burk et al., 1989). DL39TG was used for labeling p21^{ras} with [^{15}N]-isoleucine, [^{15}N]glycine, and [^{13}C]threonine together, and DL39 AvtA::Tn5 was used for all other amino acid labeling. Media containing labeled amino acids and 1 mM IPTG were inoculated to an OD of approximately 0.8 with cells from similar cultures with unlabeled amino acids. The labeled cultures were harvested after 3 h.

Isolation of p21^{ras}. Immediately after being harvested, cell pellets were resuspended in 50 mL of sonication buffer (50 mM Tris-HCl, pH 8.0 at 4 °C, 5 mM $MgCl_2$, 50 mM NaCl, 5 mM DTT, and 1 mM PMSF) and sonicated for 3 × 30 s on ice. After centrifugation at 17600*g* for 30 min, SDS–PAGE showed that most of the full-length p21^{ras} was in the pellet. The pellet was washed once in 25 mL of 30% sucrose and 5 mM EDTA (pH 7.8) and 3 times in 25 mL of 1% Triton X-100, 50 mM Tris-HCl (pH 8.0 at 4 °C), 5 mM EDTA, and 10 mM DTT. The final pellet was resuspended in 25 mL of 7 M urea buffer (7 M urea, 50 mM Tris-HCl, pH 8.0 at 4 °C, 5 mM EDTA, and 10 mM DTT) and dialyzed overnight against 850 mL of 7 M urea buffer.

The suspension of p21^{ras} was cleared by centrifugation at 25400*g* for 40 min, and the pellet was reextracted twice with 7 M urea buffer. The supernatants were assayed for protein (Bio-Rad and A_{280}), pooled, and diluted rapidly into a volume of 2 M urea buffer sufficient to produce a final A_{280} of 0.3 or less (2 M urea buffer: 2 M urea, 50 mM Tris-HCl, pH 8.0 at 4 °C, 5 mM $MgCl_2$, 50 μM GDP, and 5 mM DTT). The resulting dilute solution was dialyzed against 4–5 L of 2 M urea buffer, a similar 0.7 M urea buffer, and finally two changes of QA52 buffer (QA52 buffer: 50 mM Tris-HCl, pH 8.0 at 4 °C, 20 mM NaCl, 5 mM $MgCl_2$, 1 μM GDP, 2 mM DTT, and 0.02% azide). A total of 3 days was allowed for refolding of p21^{ras} and removal of urea. A similar folding procedure for p21^{ras} has been outlined (Casey et al., 1991).

Refolded p21^{ras} was purified by ion-exchange chromatography on QA52 resin with a 20–320 mM NaCl gradient in QA52 buffer and typically eluted in fractions with conductivities of approximately 2×10^{-4} $\mu\Omega^{-1}/cm^3$. Fractions containing essentially pure p21^{ras} based on SDS–PAGE were pooled and concentrated to approximately 15–25 mL, dialyzed against two changes of NMR buffer (NMR buffer: 20 mM Tris-HCl, pH 7.6 at room temperature, 50 mM NaCl, 5 mM DTT, 5 mM $MgCl_2$, 1 μM GDP, and 0.02% azide), concentrated to 20–30 mg/mL, and either used immediately or stored at −5 °C as 50% glycerol solutions.

Truncated p21^{ras} was often found in the sonication supernatant, the first Triton X-100 supernatant, and the pellet. Truncated p21^{ras} in the pellet was isolated, refolded, and purified in the same way as full-length p21^{ras}. p21^{ras} in the supernatants was purified separately. Two milligrams of DNase 1 was added to 50 mL of sonication supernatant, which was incubated for 10 min at room temperature, pooled with the first Triton X-100 supernatant as appropriate, and then dialyzed against two changes of QA52 buffer. p21^{ras} was purified by ion-exchange chromatography on QA52 as above, followed by gel filtration chromatography on Sephadex G-75. Fractions containing essentially pure p21^{ras} were dialyzed against NMR buffer and concentrated as before.

p21^{ras} folded by these methods binds approximately 1 stoichiometric equiv of GMPPNP. Assays kindly performed by E. Bekesi of Hoffmann-La Roche showed that our refolded p21^{ras} has GAP-dependent GTPase activity similar to that of cytosolic p21^{ras}.

Replacement of Bound GDP with GTPγS. GDP bound to approximately 10 mg of p21^{ras} was replaced with GTPγS in three cycles of dilution of p21^{ras} to 2 mL in GDP- and Mg^{2+}-free NMR buffer containing 2 mM GTPγS, and concentration to 0.45 mL using Centricon microconcentrators. EDTA was present at 3.3 mM in the first cycle and 0.8 mM in the second cycle in order to accelerate nucleotide exchange (Hall et al., 1986; Tucker et al., 1986). After each dilution with fresh GTPγS-containing buffer, p21^{ras} was incubated at room temperature for 20 min before reconcentration. Nucleotide replacement was monitored by TLC of the filtrates with which

the $p21^{ras}$ had equilibrated, using a poly(ethylenimine)–cellulose stationary phase and an aqueous 3.2% ammonium bicarbonate mobile phase. Replacement of GDP by GTPγS was approximately 80% complete by this criterion. A similar Gly-labeled truncated $p21^{ras}$ sample, in which replacement of GDP by GTPγS was shown to be more than 90% complete by precipitation of $p21^{ras}$ and HPLC, produced an NMR spectrum essentially identical to the other spectra reported here for GTPγS-bound $p21^{ras}$.

After the last concentration (from GTPγS buffer containing ≈0.16 mM residual EDTA), $p21^{ras}$ was transferred to an NMR tube, and 0.1 M $MgCl_2$ and ^2H_2O were added to produce 5 mM Mg^{2+} and 10% ^2H_2O. From the time the Mg^{2+} was added, it was approximately 44 h with the sample at approximately 13 °C before spectral features characteristic of the GDP-bound state of $p21^{ras}$ became apparent, and $p21^{ras}$-GDP comprised approximately 50% of the $p21^{ras}$ after approximately a week, as determined by NMR.

Replacement of Bound Mg^{2+} with Co^{2+}. Mg^{2+} bound to $p21^{ras}$ was replaced by Co^{2+} by removal of free Mg^{2+} from $p21^{ras}$, chelation of Mg^{2+} bound to $p21^{ras}$, and then addition of slightly substoichiometric amounts of Co^{2+}. $p21^{ras}$ was freed of excess Mg^{2+} by passage over a PD10 Sephadex G-25M size-exclusion chromatographic column equilibrated with Mg^{2+}-free NMR buffer or by dialysis against a similar buffer containing 0.2 mM $MgCl_2$. For metal replacement experiments, the buffer was NMR buffer containing 10 mM DTT and HEPES (pH 7.5 at room temperature, pH ≈8 at 4 °C) instead of Tris.

$p21^{ras}$ was incubated with a 2–3-fold molar excess of EDTA over total Mg^{2+} for 20 min at room temperature followed by at least 20 min at 4 °C. EDTA was removed by passage over a second PD10 column equilibrated with the HEPES NMR buffer; 0.4 μmol of $p21^{ras}$ (Bio-Rad assay) was diluted to a total of 5 mL containing approximately 0.2 μmol of Co^{2+} and 0.25 μmol of GDP. Only 0.2 μmol of $CoCl_2$ was added in order to avoid having Co^{2+} bind to any secondary sites that might exist and because the Bio-Rad protein assays were found to slightly overestimate the amount of $p21^{ras}$ present (C. J. Halkides, personal communication). After 8 h at 4 °C, the visible optical spectrum was taken, and $p21^{ras}$ was concentrated to approximately 1.8 mL. Co^{2+} was added to replace the amount lost in the concentration filtration effluent, and after 8 more h at 4 °C, $p21^{ras}$ was concentrated to 0.3 mL for NMR.

On the basis of the spectrum of a known concentration of Co^{2+} in buffer and the spectra of the Centricon-10 filtration effluents separated from the $p21^{ras}$, the amount of Co^{2+} lost was determined, and thus, by subtraction, the amount of Co^{2+} retained with $p21^{ras}$ was estimated. Approximately 0.17 μmol of Co^{2+} was estimated to have been retained with the 0.4 μmol of $p21^{ras}$ (estimated by the Bio-Rad assay). However, on the basis of titration of Mg^{2+}-depleted $p21^{ras}$ with increasing amounts of Mn^{2+}, the addition of only 0.3 μmol of Mn^{2+} to 0.4 μmol of $p21^{ras}$ (Bio-Rad assay) saturates a primary metal-binding site. Substoichiometric amounts of Mn^{2+} added to GDP-$p21^{ras}$ are essentially all found complexed with GDP and bound to $p21^{ras}$ (Feuerstein et al., 1987). Thus, we estimate that the above metal substitution procedure results in approximately 60% saturation of the GDP-binding site of $p21^{ras}$ with Co^{2+}. (Incomplete removal of Mg^{2+} is a likely cause of the incomplete complexation of Co^{2+} or Mn^{2+}.) Co^{2+} is specifically associated with $p21^{ras}$, as passage of the (Co^{2+})-$p21^{ras}$ over a PD10 column equilibrated with metal- and EDTA-free buffer resulted in coincident elution of $p21^{ras}$ and Co^{2+}.

NMR Spectroscopy. NMR samples contained 10% v/v ^2H_2O. Two-dimensional ^1H, ^{15}N correlation spectra, either HMQC or HSMQC (Bax et al., 1983; Zuiderweg, 1990), were obtained as described previously with JR water suppression (Campbell-Burk et al., 1989; Roy et al., 1984) on a custom-built 500-MHz spectrometer using a quadruply-tuned probe from Cryomagnet Systems (Indianapolis). Spectra were collected at 10–15 °C. Data were analyzed with minor preweighting to reduce noise from H_2O, and figures were produced using software kindly supplied by Hare Software (Woodinville WA). ^1H chemical shifts are relative to that of H_2O at 4.8 ppm, and ^{15}N chemical shifts are relative to neat $^{15}NH_3$ at 0 ppm. Differences in chemical shifts between spectra of samples prepared from different cultures and collected on different days are approximately 0.02 ppm ^1H and 0.1 ppm ^{15}N.

RESULTS

Fully-^{15}N-Labeled $p21^{ras}$. HSMQC spectra of truncated GDP $p21^{ras}$ show approximately 155 amide proton resonances (not shown). No distinctive low-field resonances are observed other than those previously identified with Gly-13 and Lys-16, at approximately 10.5 ppm in the proton dimension (Redfield & Papastavros, 1990). After replacement of GDP with GTPγS, approximately 100 resonances coincide with resonances of GDP $p21^{ras}$, but approximately 50 resonances present in the spectrum of GDP $p21^{ras}$ are absent and replaced by new resonances specific to GTPγS $p21^{ras}$. The changes seen upon substitution of GTPγS for GDP are generally noticeably greater than the differences associated with mutations of $p21^{ras}$ at position 12 (Redfield & Papastavros, 1990). Difficulties in assigning the many resonances of fully-^{15}N-labeled $p21^{ras}$, and in discerning specific changes in the spectra, lead us to concentrate on specifically-labeled samples for which simpler spectra are obtained.

Glycine Resonances. Figure 1 compares spectra of GDP- and GTPγS-bound full-length $p21^{ras}$ labeled with [^{15}N]glycine. Resonance shifts greater than the line width (0.09 ppm ^1H and 0.6 ppm ^{15}N) are interpreted to indicate changes in the environment of the amide H or N and are the focus of this paper. The peaks labeled GA, GC, GI, and GK clearly shift by more than their line widths (Table I). GA, GI, and GK have been assigned to glycines-10, -12, and -13 in the phosphate-binding loop, respectively (Campbell-Burk et al., 1989; Redfield & Papastavros, 1990). Resonances GD and GF also appear to shift slightly, but by less than their line widths.

A large peak GT at 8.4 and 110.7 ppm in full-length $p21^{ras}$ (Figure 1) is assigned to the C-terminal glycines-177, -180, and -183 because the spectrum of truncated $p21^{ras}$ lacks this peak (Figure 2). This resonance has the same proton chemical shift as the amide proton of glycine in random-coil polypeptides (Wüthrich, 1986), consistent with the C terminus of $p21^{ras}$ being disordered in crystals of full-length H-$p21^{ras}$ (Milburn et al., 1990). NMR comparisons of full-length and truncated H-$p21^{ras}$ indicated that the overall structures are similar (John et al., 1989), and we observe all the glycine resonances GA–GK of truncated N-$p21^{ras}$ in positions less than 0.1 ppm ^1H and 0.2 ppm ^{15}N away from their positions in spectra of the full-length protein.

Replacement of GDP with GTPγS in truncated $p21^{ras}$ produces the same changes in resonances GA, GC, GI, and GK as in full-length $p21^{ras}$. In truncated $p21^{ras}$, the resonance

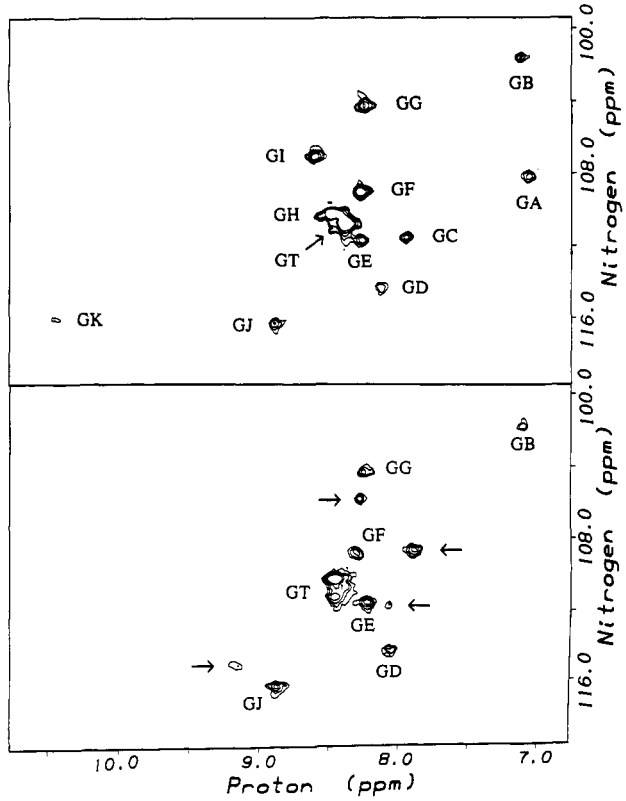

FIGURE 1: Comparison of [^{15}N]glycine-labeled full-length p21^{ras} in the GDP- and GTPγS-bound states. HMQC spectra of the amide protons are shown. The spectrum of GDP-bound p21^{ras} is in the top panel, and the spectrum of GTPγS-bound p21^{ras} is in the bottom panel.

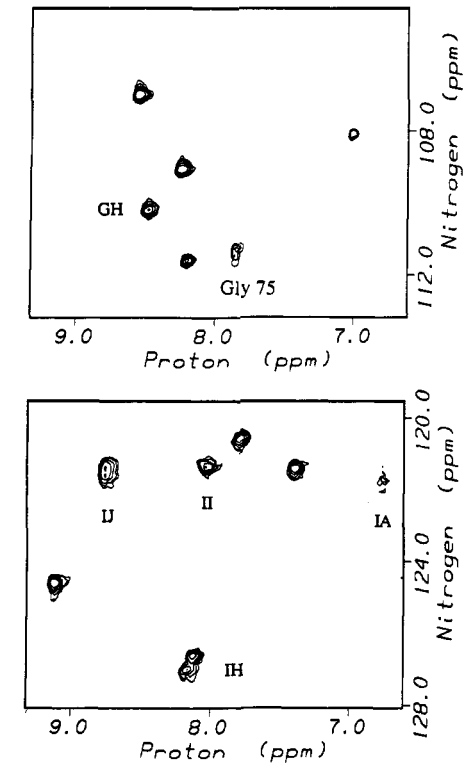

FIGURE 2: Portions of the HSMQC spectrum of truncated p21^{ras} triply labeled with [^{15}N]glycine, [^{15}N]isoleucine, and [^{13}C]threonine. The glycine region (top) shows the resonance of Gly-75 that is split by coupling to the ^{13}C in the ^{15}N dimension. The isoleucine region (bottom) shows isoleucine resonances (IA and IJ) that are split by coupling to ^{13}C in the ^{15}N dimension.

Table I: ^{1}H and ^{15}N Chemical Shifts (ppm) for Glycine Resonances in N-p21^{ras}

resonance	glycine assignment	GDP-bound p21^{ras} chemical shift		GTPγS-bound p21^{ras} chemical shift	
		^{1}H	^{15}N	^{1}H	^{15}N
GA	10[a]	7.04	108.2[b]	7.89	108.7
GB		7.16	101.7	7.12	101.8
GC	75	7.98	111.5[b]	8.08	111.6
GD	115[a]	8.12	114.2	8.06	114.1
GE		8.28	111.6	8.23	111.5
GF	60	8.30	109.0	8.32	108.8
GG		8.28	104.3	8.25	104.3
GH	15[a]	8.52	110.2[b]		
GT	177, 180, 183	8.40	110.7	8.46	110.2
GI	12[a]	8.62	107.1[b]	8.29	105.8
GJ		8.92	116.2	8.89	116.1
GK	13[a]	10.50	116.0[b]	9.18	114.9

[a] GDP-bound p21^{ras} assignments are from Campbell-Burk (1989), Campbell-Burk et al. (1989), and Redfield and Papastavros (1990) and are also based on spin-labeling of cysteine-118 to distinguish between glycines-10 and -115 (unpublished results). [b] Resonances that shift by more than the line width of 0.09 ppm ^{1}H or 0.6 ppm ^{15}N upon replacement of GDP by GTPγS. GTPγS-form resonances are not yet identified but are tentatively paired with the GDP-form resonances closest to them in chemical shift.

GH of Gly-15 in the phosphate-binding loop is clearly resolved (Figure 2), but is absent from the vicinity of its normal position, when GTPγS replaces GDP (Table I). Thus, all four glycines in the phosphate-binding loop experience different environments in the GDP- and GTPγS-bound states of p21^{ras} (resonances GA, GI, GK, and GH), as does the glycine corresponding to resonance GC.

(*A*) *Glycine-60.* In spite of the crystallographic prediction that the amide proton of Gly-60 should hydrogen-bond to the γ-phosphate of GTP (Milburn et al., 1990; Pai et al., 1990), the resonance GF that has been tentatively assigned to Gly-60 (Campbell-Burk, 1989) did not appear to shift more than its line width upon replacement of GDP with GTPγS. Gly-12 and Gly-60 are both preceded by alanine in the protein sequence, so we identified the resonance of Gly-60 by doubly labeling p21^{ras} with [^{15}N]glycine and [^{13}C$_1$]alanine. The method has been described previously (Griffey et al., 1986) but is difficult in this case because the [^{13}C]alanine was incorporated only to a level of approximately 40%, as determined by mass spectroscopy on a similar sample. Figure 3 compares spectra of [^{13}C]alanine- [^{15}N]glycine-labeled p21^{ras} collected with ^{13}C decoupling applied on and off the carbonyl frequency, to verify that broadening was due to coupling to ^{13}C. Resonances GF and GI are 21 and 23 Hz wide in the ^{15}N dimension but are narrowed to 16 and 19 Hz wide by ^{13}C decoupling. (The other resonances are not narrowed by decoupling; for example, GC is 19 Hz wide at half-height both with and without decoupling.) Thus, GF and GI correspond to glycines-12 and -60. GI is already assigned to Gly-12, so this experiment identifies resonance GF with Gly-60.

In mutant p21^{ras} in which aspartate replaces Gly-12, the resonance of Gly-60 was identified at 8.87 and 111.0 ppm by the same method (not shown).

(*B*) *Glycine-75.* Resonance GC, that is strongly sensitive to GDP replacement, remained to be identified. Gly-75 is at the end of a loop that is indicated to undergo a GMPPNP-induced conformational change (Milburn et al., 1990; Wittinghofer & Pai, 1991), so we sought to identify the resonance of Gly-75. Threonine precedes Gly-75, so p21^{ras} was labeled with [^{13}C]carbonyl and (and C$_\alpha$)-labeled threonine in addition to [^{15}N]glycine, and [^{15}N]isoleucine. Figure 2 shows that resonance GC is split by 13 Hz in the ^{15}N dimension

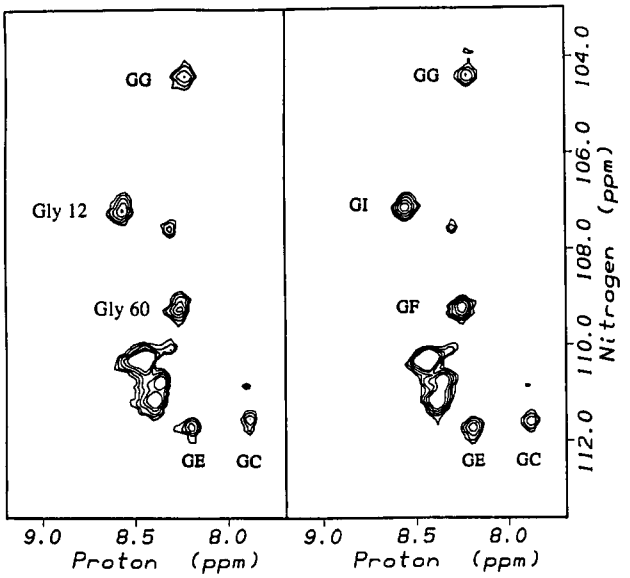

FIGURE 3: Comparison of [^{15}N]glycine and [*carbonyl*-^{13}C]alanine-labeled full-length p21^{ras}, with and without decoupling ^{13}C. HSMQC spectra of selected amide protons of p21^{ras} in the GDP-bound state are shown. The spectrum on the left was taken without decoupling [^{13}C]carbonyl, and the spectrum on the right was taken with decoupling. Coupling between amide nitrogens and ^{13}C is evident as slight broadening in the ^{15}N dimension that is abolished by decoupling ^{13}C.

specifically. The doublet structure collapses upon ^{13}C decoupling, and thus identifies resonance GC with Gly-75.

Isoleucine Resonances. Figure 2 also shows that two isoleucine resonances IA and IJ are split in the ^{15}N dimension by [$^{13}C_1$]threonine. The contours displayed in Figure 2 cut through the top of resonance IA where its two components are visible as distinct companion peaks with the same proton chemical shift, but the contour that unites them as a single (split) peak appears clearly at a slightly lower threshold. Narrowing of resonance IA was not clearly observed in a [^{13}C]carbonyl-decoupled spectrum because of an equipment malfunction, but narrowing of IJ was obvious. In Figure 2, IH is also composed of two components, but these differ in both the ^{15}N and ^{1}H dimensions, and they do not collapse into a single resonance upon ^{13}C decoupling. In a sampling of different [^{15}N]isoleucine-labeled p21^{ras} preparations, IH sometimes consisted of two components even though threonine was not labeled, and IA was often weak. Thus, the splitting of IA and IJ specifically in the ^{15}N dimension identifies them collectively with isoleucines-21 and -36, which follow threonine in the amino acid sequence. Resonance IE was identified in the same way, using a sample labeled with [$^{13}C_1$]leucine and [^{15}N]isoleucine, as arising from Ile-24.

Replacement of GDP by GTPγS. Figure 4 shows the HMQC spectra of [^{15}N]isoleucine-labeled p21^{ras} in the GDP- and GTPγS-bound states (top and bottom, respectively). Upon replacement of GDP by GTPγS, resonances IB and IE appear to shift slightly by less than the line width, and three resonances, IA, IC, and IJ, are shifted to new positions. Two new peaks can be observed with certainty in GTPγS–p21^{ras} (Table II). A GTPγS-specific peak may not be easily observed for the third responsive isoleucine either because the resonance occurs at a low chemical shift where the JR-detected spectra are insensitive and there is interference from H_2O or because multiple conformations exist and interconvert at rates comparable to the frequency separation between the corresponding resonances. The fact that resonances IA and IJ shift indicates that isoleucines-21 and -36 are strongly affected by the conformational change.

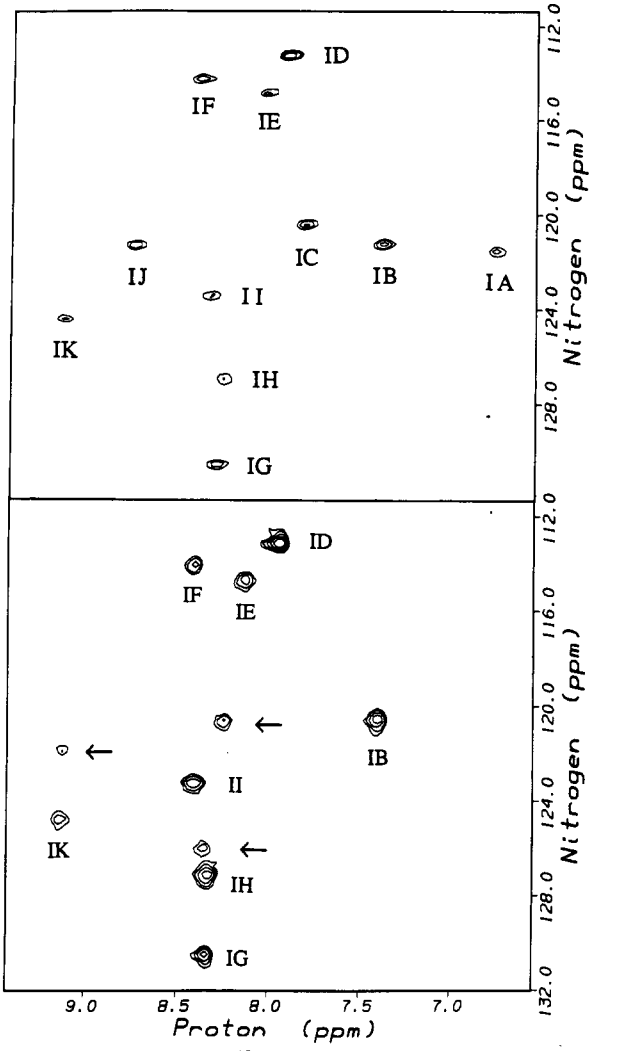

FIGURE 4: Comparison of [^{15}N]isoleucine-labeled p21^{ras} in the GDP- and GTPγS-bound states. HMQC spectra of the amide protons are shown. The spectrum of GDP-bound p21^{ras} is on the top, and the spectrum of GTPγS-bound p21^{ras} is on the bottom.

Table II: ^{1}H and ^{15}N Chemical Shifts (ppm) for Isoleucine Resonances in p21^{ras}

resonance	isoleucine assignments	GDP-bound p21^{ras} chemical shift		GTPγS-bound p21^{ras} chemical shift	
		^{1}H	^{15}N	^{1}H	^{15}N
IA	36	6.79	121.8[a]	8.38	126.2
IB		7.45	121.5	7.41	120.8
IC		7.87	120.8[a]	8.25	120.8
ID		7.95	113.6	7.97	113.4
IE	24	8.07	115.1	8.15	115.0
IF		8.44	114.6	8.43	114.4
IG		8.35	130.8	8.37	130.8
IH		8.31	127.1	8.35	127.4
II	163	8.41	123.7	8.43	123.5
IJ	21	8.81	121.6[a]	9.15	122.1
IK		9.20	124.7	9.17	125.1

[a] Resonances that shift by more than the line width of 0.09 ppm ^{1}H or 0.6 ppm ^{15}N upon replacement of GDP by GTPγS. GTPγS-form resonances are not yet identified but are tentatively paired with the GDP-form resonances closest to them.

Truncated and full-length p21^{ras} labeled with [^{15}N]isoleucine were also compared. Only isoleucine resonance II appears at a different position in full-length (8.41 and 123.7 ppm) and truncated p21^{ras} (8.04 and 121.4 ppm, compare Figure 4 with Figure 2). Because the isoleucine closest to the C-terminus both in space and in the amino acid sequence of p21^{ras} is Ile-163, we tentatively assign resonance II to Ile-163.

This resonance is insensitive to replacement of GDP by GTPγS in both full-length and truncated p21^{ras}.

Replacement of Mg^{2+} by Co^{2+} in p21^{ras}. In order to determine which of resonances IA and IJ corresponds to Ile-36, we took advantage of the fact that the amide of Ile-36 is much closer to the metal (6 Å) than that of Ile-21 (8.5 Å) based on coordinates of p21^{ras} bound to GDP kindly supplied by I. Schlichting (Schlichting et al., 1990). Protons close to a paramagnetic ion are subject to paramagnetically-enhanced longitudinal and transverse relaxation, and the extent to which proton resonances are relaxed depends on the distance to the paramagnet, the correlation time of the paramagnetic complex, and, in the case of Co^{2+}, the direction of the Co^{2+}-to-proton vector relative to the coordination geometry of Co^{2+}.

We are directly observing the protein bound to the paramagnetic ion. p21^{ras} forms a high-affinity slow-exchange complex with Mg^{2+} [see Reinstein et al. (1991)], and a high proportion of the enzyme is maintained in the metal-bound form without a large amount of the metal free in solution or nonspecifically bound. We have avoided nonspecific binding at the expense of not completely saturating the principle metal-binding site. Metal-binding titrations and the coelution of Co^{2+} and p21^{ras} upon gel filtration indicate that the complex between p21^{ras} and one Co^{2+} is the major species present, although a significant residual population of Co^{2+}-free p21^{ras} is also present.

For the protons that we are interested in, close to the metal but not bound to it, the dipolar paramagnetic contribution to the transverse relaxation rate of a nuclear spin species dominates and is given by

$$R_2' = \frac{\gamma_I^2 g^2 S(S+1)\beta^2}{15r^6}\left(4\tau_c + \frac{3\tau_c}{1+\omega_I^2\tau_c^2} + \frac{13\tau_c}{1+\omega_S^2\tau_c^2}\right) \quad (1)$$

where γ_I is the gyromagnetic ratio of the NMR nucleus (^1H or ^{15}N here), g and S are the g value and spin of the unpaired electrons of Co^{2+}, respectively, β is the Bohr magneton, ω_I is the Larmor frequency of the NMR nucleus, ω_S is the electron spin resonance frequency of the paramagnetic ion, and τ_c is the correlation time of the metal complex. The correlation time depends on the rate of electron spin relaxation, the tumbling rate of the complex, and the dissociation rate of Co^{2+} from p21^{ras}. For Co^{2+}, the electron spin relaxation rate is on the order of 10^{12} s^{-1} and dominates the other two contributions, even assuming a dissociation rate hundreds of times that of Mg^{2+} [see Reinstein et al. (1991)].

Since paramagnetically-induced nuclear relaxation varies with the inverse of the sixth power of distance, it is important only for protons near the metal. We chose to use Co^{2+} because its short correlation time limits paramagnetic effects to relatively short distances. During the pulse sequence, the magnetization decreases exponentially during the two HMQC intervals, $\tau_J \approx 1/2J_{NH}$, at a rate equal to the proton transverse relaxation rate. In addition, the amplitude (height) of the resonance observed decreases in proportion to the transverse relaxation rate during the ^{15}N and ^1H evolution time and the free induction decay, essentially reflecting increases in the ^{15}N and ^1H line widths. Thus, we expect that

$$A'/A = \left(\frac{R_2}{R_2 + R_2'}\right)\left(\frac{R_D}{R_D + R_D'}\right)\exp(-2\tau_J R_D') \quad (2)$$

where A and A' are the resonance heights in Mg^{2+} and Co^{2+} p21^{ras}, R_2 and R_D are the proton transverse relaxation rate and double-quantum (^{15}N–^1H) relaxation rate for Mg^{2+} p21^{ras},

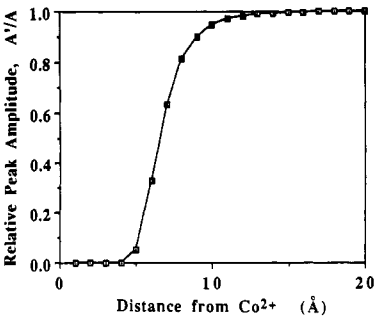

FIGURE 5: Theoretical distance dependence of reduction in signal amplitude due to paramagnetically-enhanced relaxation in the presence of Co^{2+} (eq 3).

respectively, and the primed symbols R_2' and R_D' denote the additional paramagnetic contributions to these relaxation rates in the paramagnetic protein complex. The rates R_2 and R_D are the inverse of the transverse relaxation times, and are equal to π times the HMQC line widths in the proton and ^{15}N dimensions, respectively. R_D and R_D' are approximately the sums of the transverse relaxation rates for protons and ^{15}N. Proton relaxation dominates R_D', so R_D' is approximately equal to R_2', and the dependence on the distance to ^{15}N can be neglected relative to the dependence on the distance to the amide proton. From eq 2, we obtain

$$A'/A = \frac{\exp[-0.009(11.7\text{ Å}/r)^6]}{[1 + 0.006(11.7\text{ Å}/r)^6][1 + 0.007(11.7\text{ Å}/r)^6]} \quad (3)$$

where r is the distance between the proton and the metal ion in angstroms. To obtain eq 3, we assume $\tau_c = 2 \times 10^{-12}$ s (Melamud & Mildvan, 1975). Experimental values of R_2 and R_D are used, τ_J was 4.5 ms in all our experiments, and an average value of $g^2 = 11$ was obtained by EPR. The r^{-6} dependence of the rates makes the exact choice of g and τ_c relatively unimportant. Two-fold differences in g or τ_c introduce 12% errors in the predicted distance dependence. Figure 5 shows the distance dependence of the relative resonance amplitude in the presence of Co^{2+} predicted by eq 3. Resonances of protons 6 Å or less from Co^{2+} are predicted to be reduced to less than a third of their normal amplitudes whereas resonances of protons further than 9 Å from Co^{2+} should retain more than 90% of their normal amplitude, neglecting any orientation dependence (anisotropy).

The anisotropy of relaxation by Co^{2+} was estimated to introduce a distance uncertainty of approximately 1 Å based on the effect of Co^{2+} substitution on the resonances of glycines surrounding the metal site at distances known from the crystal structure of p21^{ras}. On the basis of Co^{2+}-substituted glycine-labeled p21^{ras}, Ile-36 is expected to be severely attenuated in the presence of Co^{2+}, and Ile-21 might be attenuated, but should remain easily observable.

Comparison of spectra of Mg^{2+}- and Co^{2+}-containing [^{15}N]-isoleucine-labeled p21^{ras} indicates that the overall structure of p21^{ras} is preserved since 10 of the 11 resonances occur in their normal positions (Figure 6). However, one resonance, IA, is absent and not replaced by any new resonances. IK is also attenuated by Co^{2+}, but less than IA, and IK cannot correspond to Ile-36 because it was not split by coupling to [^{13}C]threonine. IA is one of the two resonances identified as Ile-21 and Ile-36. Therefore, we assign resonance IA to Ile-36 and resonance IJ to Ile-21.

Upon replacement of Mg^{2+} by Co^{2+} in glycine-labeled p21^{ras}, resonance GC is reduced in intensity by a factor of at least 2, and a new resonance appears at 7.83 and 108.9 ppm (not

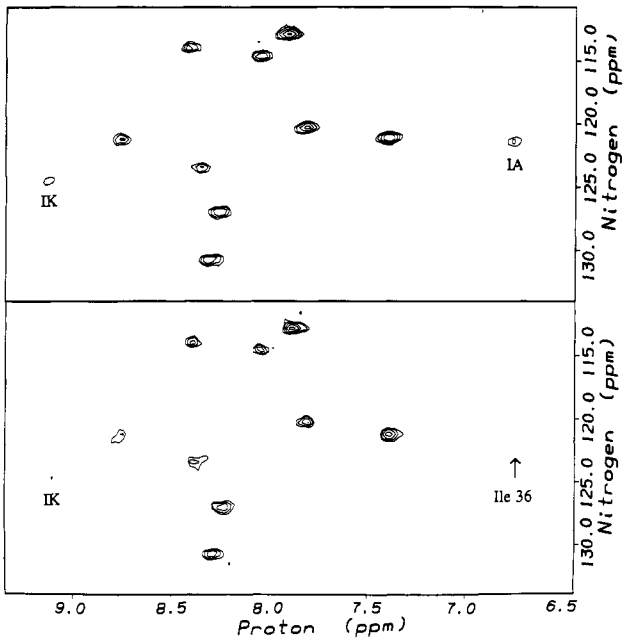

FIGURE 6: Comparison of HMQC spectra of [^{15}N]isoleucine-labeled p21^{ras} containing Mg^{2+} (top) and Co^{2+} (bottom).

shown). Both of these changes are also observed when GTPγS replaces GDP. The reduction in intensity of resonance GC is more likely due to a conformational change (and a residual population of Co^{2+}-free p21^{ras}) than to paramagnetic effects because Gly-75 is approximately 17 Å from the metal ion. Replacement of Mg^{2+} by Co^{2+} does not produce all the spectral changes associated with the GTPγS-bound state, as the resonance of Gly-12 remains in its GDP-specific position. Nonetheless, a similar disappearance of resonance GC and appearance of a resonance at 7.85 and 108.9 ppm were also observed when Mg^{2+} was replaced by Mn^{2+} (not shown), so these preliminary metal ion replacement experiments indicate that some of the regions of p21^{ras} that are affected by replacement of GDP by GTPγS are also affected by the metal ion.

DISCUSSION

Approximately one-third of the amide resonances of truncated p21^{ras} are replaced by different resonances upon replacement of GDP by GTPγS. The chemical shifts of protons are extremely sensitive to changes in environment, so it is possibly more significant that two-thirds of the resonances appear unaffected (barring exact exchanges of positions). This indicates that large portions of the structure of p21^{ras} are unperturbed by exchange of the nucleotides.

Crystallographic studies indicate that roughly 28 out of 166 residues move significantly upon replacement of GDP by GTP analogs [see Milburn et al. (1990) and Schlichting et al. (1990)], yet a larger proportion of the amide proton resonances are affected. This may be because NMR will detect changes in the environments of both the residues that move and the residues whose environments are changed as a result. Thus, NMR provides a very comprehensive assessment of the impact of the conformational change on different residues of the protein. For example, it is possible that one function of the conformational change is to unmask stationary but previously inaccessible residues and thus enable them to interact with GAP in the GTP-bound state of p21^{ras}.

In [^{15}N]glycine-labeled p21^{ras}, five resonances shift dramatically upon replacement of GDP by GTPγS, but we have only found four new resonances in the GTPγS-bound state. The four resonances specific to GTPγS-bound p21^{ras} have possible counterparts among the GDP-specific resonances having different proton chemical shifts but similar ^{15}N chemical shifts. Similarly, in [^{15}N]isoleucine-labeled p21^{ras}, two of the three GTPγS-specific resonances can be tentatively paired with two nearby GDP-specific resonances at similar ^{15}N chemical shifts. Thus, the chemical shift of ^{15}N may be dominated by factors that are relatively insensitive to the conformational change, such as covalent bonding interactions. By pairing resonances lost from the GDP-bound spectrum with nearby new resonances arising in the GTPγS-bound spectrum with similar ^{15}N chemical shifts, the GTPγS-specific resonances can be tentatively identified with specific glycine assignments in GDP-bound p21^{ras}, as in Table I.

The most dramatic resonance shift observed in [^{15}N]glycine-labeled p21^{ras} is that of Gly-13, which hydrogen-bonds to a terminal oxygen in GDP but to the β–γ-bridging oxygen in GTP (Tong et al., 1989; Pai et al., 1990). It is not surprising that glycines-15 and -10 should also respond to replacement of GDP by GTPγS. Both are proposed to interact directly or indirectly with the β- or γ-phosphate of GMPPNP (Pai et al., 1989, 1990) although neither has the higher than average chemical shift that would be expected from a proton in a strong hydrogen bond to phosphate. The sensitivity of Gly-12 to replacement of GDP by GTPγS can be explained by proximity to Gly-13.

In the crystal structures, Gly-60 appears to hydrogen-bond to the γ-phosphate of GTP analogs (Milburn et al., 1990; Pai et al., 1989). In addition, the equivalent of Gly-60 in the α-subunit of the heterotrimeric G-protein G_α is required for the GTP-induced conformational change (Miller et al., 1988) as is the equivalent residue in EF-Tu (Hwang et al., 1990). Nevertheless, our data appear to indicate that the Gly-60 resonance is not sensitive to substitution of GTP by GTPγS. This inference, if correct, would suggest that Gly-60 does not hydrogen bond to the γ-phosphate group of GTPγS, in contrast to expectations from the X-ray models for GMPPNP and GMPPCP. The sulfur group might fail to accept the hydrogen bond from the Gly-60 amide (Gregoret et al., 1992). However, this inference is premature, because we have positively identified the resonance at this position with Gly-60 only in the GDP form, and not in the GTPγS form. The resonance in question is in a central region of the spectrum, to which another glycine resonance might well shift in the GTPγS form.

In mutant p21^{ras} in which aspartate replaces Gly-12, the resonance of Gly-60 is significantly shifted relative to wild-type p21^{ras}. This is consistent with the crystallographic observation that when valine replaces Gly-12, the side chain of valine interferes sterically with residues 60 and 61 (Krengel et al., 1990). On the basis of the positions and orientations of residue 12 and Gly-60, it should be possible for the side chain of Asp-12 to hydrogen-bond with the amide of Gly-60, consistent with the downfield shift of Gly-60 in the Asp-12 mutant.

Replacement of Mg^{2+} by either Mn^{2+} or Co^{2+} caused the resonance corresponding to Gly-75 to shift, and a new resonance to appear at a similar position to that of a resonance produced by GTPγS binding. Studies of crystals of Mn^{2+} p21^{ras} also indicate that the protein conformation is different from Mg^{2+} p21^{ras} (Wittinghofer & Pai, 1991). The Mg^{2+} ion can only represent part of the conformational coupling mechanism, because its replacement by Mn^{2+} or Co^{2+} does not affect at least one residue, Gly-12, that is affected by nucleotide replacement. However, the similarity of the effect

on Gly-75 produced by both metal and nucleotide replacement suggests that the metal could play a role in mediating the conformational change that results from replacement of GDP by GTPγS.

We have now identified the resonances of glycines-10, -12, -13, -15, -60, -75, and -115. The remaining four glycine resonances in the truncated form must belong to glycines-48, -77, -138, and -151, and they shift less than 0.05 ppm upon nucleotide replacement. Thus, the nucleotide-induced conformational change appears to extend to Gly-75 but not to Gly-77 in solution, as in the crystals (Milburn et al., 1990; Wittinghofer & Pai, 1991). The glycines at positions 75 and 77 might serve as swivel points and uncouple the motion of the 60–76 loop and helix region from the residues beyond (Fasano et al., 1988; Jurnak et al., 1990).

In addition to glycines-60 and -75, we have identified the amide resonances of isoleucines-21, -24, and -36. The sensitivity of the resonance of Ile-36 to replacement of GDP by GTPγS agrees with the crystallographic studies in indicating that the effector-binding loop is conformationally coupled to the identity of the bound nucleotide (Milburn et al., 1990; Wittinghofer & Pai, 1991). The resonance of Ile-36 could be a valuable probe of GAP and effector binding as well, as these are believed to bind to p21^{ras} near Ile-36 (Adari et al., 1988; Calés et al., 1988; Sigal et al., 1986; Willumsen et al., 1986). Crystallographic studies did not predict effects on the α-helix in which Ile-21 resides. Conformational effects on this helix are nevertheless expected, considering that the helix dipole has been proposed to stabilize binding of the negatively charged phosphates of GDP and GTP (Hol et al., 1978).

The isoleucine resonance IC that responds strongly to replacement of GDP by GTPγS could correspond to Ile-55 in the β-sheet, which undergoes a conformational change upon replacement of GDP by GTPγS (Yamasaki et al., 1989).

On the basis of the relative insensitivity of glycines-48, -77, -138, and -151 and (tentatively) Ile-163 to replacement of GDP by GTPγS, it seems improbable that the conformational change affects the side of p21^{ras} that faces away from the nucleotide-binding site, and the C-terminus. This result is interesting in view of evidence that regions of G_α analogous to the C-terminal helix region of p21^{ras} are involved in binding to receptors specifically when G_α is bound to GDP (Sullivan et al., 1987).

ACKNOWLEDGMENT

We thank D. LeMaster for the gift of *E. coli* strain DL39TG, F. McCormick and J. A. Noble for plasmids, and C. J. Halkides for helpful discussions on the synthesis of threonine as well as generous assistance with mass spectroscopy. We are also grateful to S. Campbell-Burk for a useful discussion.

REFERENCES

Adari, H., Lowy, D. R., Willumsen, B. M., Der, C. J., & McCormick, F. (1988) *Science 240*, 518–521.

Amann, E., & Brosius, J. (1985) *Gene 40*, 183–190.

Amann, E., Ochs, B., & Abel, K.-J. (1988) *Gene 69*, 301–315.

Barbacid, M. (1987) *Annu. Rev. Biochem. 56*, 799–827.

Bax, A., Griffey, R. H., & Hawkins, B. L. (1983) *J. Magn. Reson. 55*, 301–315.

Bos, J. L., Toksoz, D., Marshall, C. J., Verlaan-de Vries, Veeneman, G. H., van der Eb, A. J., van Boom, J. H., Janssen, J. W. G., & Steenvoorden, A. C. M. (1985) *Nature 315*, 726–730.

Bourne, H. R., Sanders, D. A., & McCormick, F. (1990) *Nature 348*, 125–132.

Bourne, H. R., Sanders, D. A., & McCormick, F. (1991) *Nature 349*, 117–127.

Calés, C., Hancock, J. F., Marshall, C. J., & Hall, A. (1988) *Nature 332*, 548–551.

Campbell-Burk, S. (1989) *Biochemistry 28*, 9478–9484.

Campbell-Burk, S., Papastavros, M. Z., McCormick, F., & Redfield, A. G. (1989) *Proc. Natl. Acad. Sci. U.S.A. 86*, 817–820.

Casey, P. J., Thissen, J. A., & Moomaw, J. F. (1991) *Proc. Natl. Acad. Sci. U.S.A. 88*, 8631–8635.

Fasano, O., Aldrich, T., Tamanoi, F., Taparowski, E., Furth, M., & Wigler, M. (1984) *Proc. Natl. Acad. Sci. U.S.A. 81*, 4008–4013.

Fasano, O., Crechet, J. B., De Vendittis, E., Zahn, R., Feger, G., Vitelli, A., & Parmeggiani, A. (1988) *EMBO J. 7*, 3375–3383.

Field, J., Broek, D., Kataoka, T., & Wigler, M. (1987) *Mol. Cell. Biol. 7*, 2128–2133.

Feuerstein, J., Kalbitzer, H. R., John, J., Goody, R. S., & Wittinghofer, A. (1987) *Eur. J. Biochem. 162*, 49–55.

Feuerstein, J., Goody, R. S., & Webb, M. R. (1989) *J. Biol. Chem. 264*, 6188–6190.

Gregoret, L. M., Rader, S. D., Fletterick, R. J., & Cohen, F. E. (1991) *Proteins: Struct., Funct., Genet. 9*, 99–107.

Griffey, R. H., Redfield, A. G., McIntosh, L. P., Oas, T. G., & Dahlquist, F. W. (1986) *J. Am. Chem. Soc. 108*, 6816–6817.

Griffey, R. H., & Redfield, A. G. (1987) *Q. Rev. Biophys. 19*, 51–82.

Hall, A., & Self, A. J. (1986) *J. Biol. Chem. 261*, 10963–10965.

Hanahan, D. (1983) *J. Mol. Biol. 166*, 557–580.

Hol, W. G. J., van Duijnene, P. T., & Berendsen, H. J. C. (1978) *Nature 273*, 443–446.

Hwang, Y. W., Jurnak, F., & Miller, D. L. (1990) in *The Guanine-Nucleotide Binding Proteins: Common Structural and Functional Properties* (Bosch, L., Kraal, B., & Parmeggiani, A., Eds.) Plenum Press, New York.

John, K., Schlichting, I., Schiltz, E., Rösch, P., & Wittinghofer, A. (1989) *J. Biol. Chem. 264*, 13086–13092.

Jurnak, F., Heffron, S., & Bergmann, E. (1990) *Cell 60*, 525–528.

Krengel, U., Schlichting, I., Scherer, A., Schumann, R., French, M., John, J., Kabsch, W., Pai, E. F., & Wittinghofer, A. (1990) *Cell 62*, 539–548.

LeMaster, D. M., & Richards, F. M. (1988) *Biochemistry 27*, 142–150.

Lowry, D. F., Ahmadian, M. R., Redfield, A. G., & Sprinzl, M. (1992) *Biochemistry 31*, 2977–2982.

Melamud, E., & Mildvan, A. S. (1975) *J. Biol. Chem. 250*, 8193–8201.

Milburn, M. V., Tong, L., deVos, A. M., Brünger, A., Yamaizumi, Z., Nishimura, S., & Kim, S.-H. (1990) *Science 247*, 939–945.

Miller, R. T., Masters, S. B., Sullivan, K. A., Beiderman, B., & Bourne, H. R. (1988) *Nature 334*, 712–715.

Muchmore, D. C., McIntosh, L. P., Russell, C. B., Anderson, D. E., & Dahlquist, F. W. (1989) *Methods Enzymol. 177*, 44–73.

Nishimura, S., & Sekiya, T. (1987) *Biochem. J. 243*, 313–327.

Pai, E. F., Kabsch, W., Krengel, U., Holmes, K. E., John, J., & Wittinghofer, A. (1989) *Nature 341*, 209–214.

Pai, E. F., Krengel, U., Petsko, G. A., Goody, R. S., Kabsch, W., & Wittinghofer, A. (1990) *EMBO J. 9*, 2351–2359.

Redfield, A. R., & Papastavros, M. Z. (1990) *Biochemistry 29*, 3509–3514.

Reinstein, J., Schlichting, I., Frech, M., Goody, R. S., & Wittinghofer, A. (1991) *J. Biol. Chem. 266*, 17700–17706.

Roy, S., Papastavros, M. Z., Sanchez, V., & Redfield, A. G. (1984) *Biochemistry 23*, 4395–4400.

Sato, M., Okawa, K., & Akabori, S. (1957) *Bull. Chem. Soc. Jpn. 30*, 937–938.

Schlichting, I., Almo, S. C., Rapp, G., Wilson, K., Petratos, K., Lentfer, A., Wittinghofer, A., Kabsch, W., Pai, E. F., Petsko, G. A., & Goody, R. S. (1990) *Nature 345*, 309–315.

Seeburg, P. H., Colby, W. W., Capon, D. J., Goeddel, D. V., & Levinson, A. D. (1984) *Nature 312*, 71–75.
Sigal, I. S., Gibbs, J. B., D'Alonzo, J. S., & Scolnik, E. M. (1986) *Proc. Natl. Acad. Sci. U.S.A. 83*, 4725–4729.
Smithers, G. W., Poe, M., Latwesen, D. G., & Reed, G. H. (1990) *Arch. Biochem. Biophys. 280*, 416–420.
Sullivan, K. A., Miller, R. T., Masters, S. B., Beiderman, B., Heideman, W., & Bourne, H. R. (1987) *Nature 330*, 758–760.
Tong, L., Milburn, M. V., deVos, A. M., & Kim, S.-H. (1989) *Science 245*, 244.
Trahey, M., & McCormick, F. (1987) *Science 238*, 542–545.
Tucker, J., Sczakiel, G., Feuestein, J., John, J., Goody, R. S., & Wittinghofer, A. (1986) *EMBO J. 5*, 1351–1358.
Vogel, U. S., Dixon, R. A. F., Schaber, M. D., Diehl, R. E., Marshall, M. S., Scolnick, E. M., Sigal, I. S., & Gibbs, J. B. (1988) *Nature 335*, 90–93.
West, M., Kung, H., & Kamata, T. (1990) *FEBS Lett. 259*, 245–248.
Willumsen, B. M., Papageorge, A. G., Kung, H.-F., Bekesi, E., Robins, T., Johnsen, M., Vass, W. C., & Lowy, D. R. (1986) *Mol. Cell. Biol. 6*, 2646–2654.
Wittinghofer, A., & Pai, E. F. (1991) *Trends Biochem. Sci. (Pers. Ed.) 16*, 382–387.
Wolfman, A., & Macara, I. G. (1990) *Science 248*, 67–69.
Wüthrich, K. (1986) *NMR of Proteins and Nucleic Acids*, Wiley, New York.
Yamasaki, K., Kawai, G., Ito, Y., Muto, Y., Fujita, J., Miyazawa, T., Nishimura, S., & Yokoyama, S. (1989) *Biochem. Biophys. Res. Commun. 162*, 1054–1062.
Zuiderweg, E. R. P. (1990) *J. Magn. Reson. 86*, 346–357.

Registry No. GDP, 146-91-8; GTP, 86-01-1; Gly, 56-40-6; Ile, 73-32-5.